TEXTILE topics

Volume 2003-3
Summer 2003

International Textile Center | Texas Tech University | Lubbock, Texas USA

IMPORTANT ANNOUNCEMENT

Please be aware that this is **the final** printed version of *Textile Topics* you will receive. Due to escalating printing and postage costs, we have decided to publish *Textile Topics* in an electronic format only (e-mail). This will allow us to keep this publication **free** to our readers and help us conserve financial resources for research purposes.

If you have not done so, please do the following:

Please send your e-mail address to: **TextileTopics@ttu.edu**

In the subject line type:
Subscribe Textile Topics

In the body of the e-mail type:
Your Name
Company Name
Address

If you have any questions regarding this announcement, please e-mail us at **TextileTopics@ttu.edu**
Thank you for your attention in this matter.

Sharing current research information and trends in the fiber and textile industries.

International Textile Center
Texas Tech University
Lubbock, Texas
79409 - 5019
phone 806.747. 3790
fax 806.747. 3796
itc@ttu.edu
http://www.itc.ttu.edu

TEXAS INTERNATIONAL COTTON SCHOOL

The next session of the Texas International Cotton School will be held October 6-17, 2003. It is not too late to enroll for this session. Students atttending can expect to gain a better understanding of US cotton production, processing, testing techniques, and marketing systems. More information can be obtained from Mandy Howell, Lubbock Cotton Exchange, 806-763-4646 or e-mail LCEcotton@aol.com.

ITC TRAVEL

- Dean Ethridge to Irving, Texas to attend the Texas Cotton Association 92nd Annual Convention, April 24-26.
- Eric Hequet and Dean Ethridge to Greenville, South Carolina to attend the 16th Annual EFS (Engineered Fiber Selections) Conference, June 9-13.
- Dean Ethridge to Austin, Texas to attend the Texas Department of Agriculture Advisory Committee Meeting, June 17.
- Noureddine Abidi and Eric Hequet to Cary, North Carolina to visit with personnel from Cotton Incorporated about current and future research projects.

PRELIMINARY VALIDATION OF A FABRIC SMOOTHNESS ASSESSMENT SYSTEM

Christopher N. Turner (Corresponding Author)
Hamed Sari-Sarraf
Eric F. Hequet
Sunho Lee

Cotton Incorporated and The Texas Food and Fiber Commission funded the research reported here.
This article was reprinted with permission from SPIE and originally presented at the Sixth International Conference on Quality Control by Artificial Vision, Vol. 5132, pp. 140-148 (2003).

ABSTRACT

A fabric's tendency to wrinkle is vitally important to the textile industry as it impacts the visual appeal of apparels. Current methods of grading this characteristic, called fabric smoothness, are very subjective and inadequate. As such, a quantitative method for assessing fabric smoothness is of the utmost importance to the textile community. To that end, we have proposed a laser-based surface profiling system that utilizes a smart camera to sense the 3-D topography of the fabric specimens. The system incorporates methods based on anisotropic diffusion and the facet model for characterizing edge information that ultimately relate to a specimen's degree of wrinkling. In this paper, we detail the initial steps in a large-scale validation of this system. Using histograms of the extracted features, we compare the output of the system among 78 swatches of various color, type, and texture. The results show consistency among repeated scans of the same swatch as well as among different swatches taken from the same fabric sample. The fact that swatches taken from same piece of fabric typically wrinkle similarly adds to the feasibility of the system. In other words, it adequately identifies and measures appropriate features of the wrinkles found on a sample.

INTRODUCTION

The overall quality of a fabric is dependent on a number of factors, including tensile strength, shrinkage, abrasion resistance, and fabric construction. Also among these is the fabric's tendency to wrinkle after home laundering – referred to as smoothness. The protocol for ascertaining smoothness grade of a fabric is outlined in the American Association of Textile Chemists and Colorists (AATCC) Test Method (TM) 124[1]. This standard test is designed to evaluate the smoothness of fabric specimens after repeated home laundering. Once three specimens, called *swatches*, per fabric have been through 5 standard washing-drying cycles, three technicians visually evaluate them. For these evaluations, the specimen is laid on a solid surface that stands at an incline of 5 degrees from vertical under specified lighting conditions. The specimen is then compared to six standard replicas, which are 3-D plastic models, showing varying degrees of smoothness (Figure 1) and having grades 1 (very wrinkly), 2, 3, 3.5, 4, and 5 (very smooth). The specimen is assigned the grade of the replica it most closely resembles.

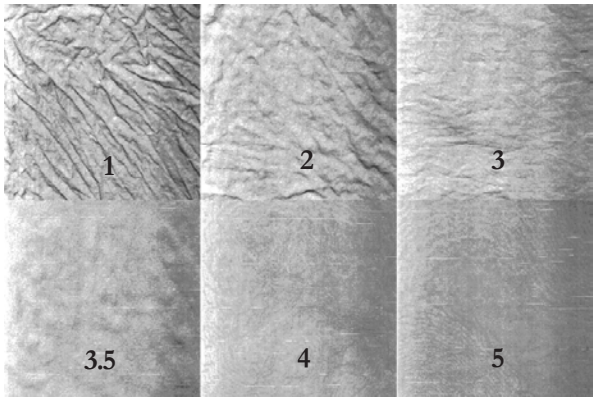

Figure 1 - Images of the six replicas

Beside exhibiting inter- and intra-subject variability and being an expensive process, the current smoothness grading system is very inadequate in its ability to provide a true surface description of the fabric. It is, therefore, desirable to develop a system to accurately quantify surface smoothness in a practical and repeatable manner.

Previous research efforts have focused on this goal with limited success. These works include ascertaining fabric smoothness by observing surface and shade area ratios from images obtained from a color flatbed scanner[2], using laser-triangulation with a rotating stage and neural network classifier[3], as well as using stereo imaging with fractal geometry[4]. Although interesting in their own right, these systems either fail to capture or to describe the 3-D nature of wrinkles and creases that ultimately characterize the fabric's degree of smoothness.

In a previous work we introduced a system based on a smart CMOS camera combined with a laser-line projector to obtain range images of fabric samples[5]. Because these range images provide an excellent depiction of the surface topography of fabric specimens, by using the *facet model*[6] and the *integrated directional derivative gradient* (IDDG) *operator*[7], we can locate and quantitatively describe various types of wrinkles using cross-sectional wrinkle profiles. In this paper, we present our to-date progress in the design, development, and testing of this system and outline the preliminary steps towards a large-scale validation of its performance. To that end, results of the

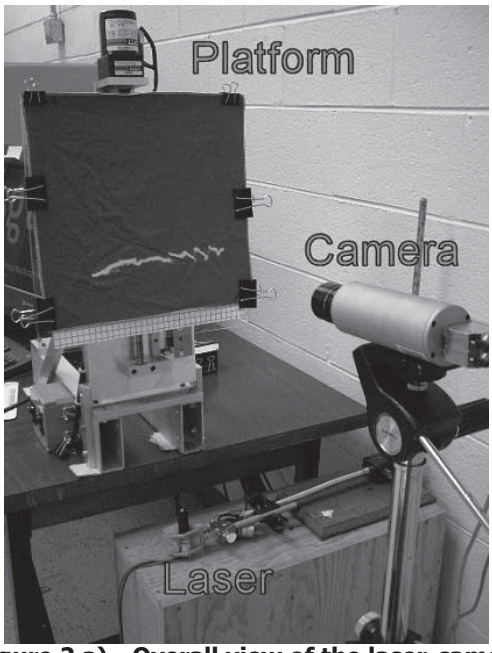

Figure 2 a) - Overall view of the laser-camera image acquisition system

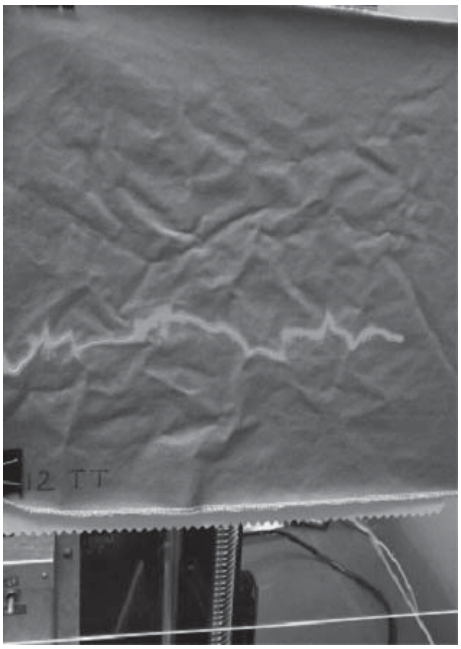

Figure 2 b) - Laser line being projected onto a sample fabric.

application of the proposed system to three swatches from each of 26 sample fabrics are presented and analyzed.

SYSTEM OVERVIEW

Image Acquisition

The image acquisition system (Figure 2a) consists of a sheet-of-light, laser-line projector; a smart CMOS camera; a moving platform; and a PC. The laser is a 600-700 nm, 5 mW solid-state device with a line generation optic. The laser line is projected at a low angle (around 5 degrees) onto the moving platform where a swatch is placed. The camera is positioned directly above the platform so that its line of sight is perpendicular to the plane of motion. As the fabric swatch is moved across the laser line, the camera records the location of the line on the swatch. Bumps, wrinkles, and creases in the fabric distort the laser line, Figure 2(b). During each time step, the camera records these distortions by sensing the row location of the center of the laser line in each column. These values are combined to produce a range image of the scanned swatch. Simultaneously, the camera also records intensity along the laser line, producing an accompanying intensity image. Using this system, we image an 8in. x 8in. section from the center of a 15in. x 15in. swatch at approximately 40 μm per gray level range resolution and 400 μm per pixel resolution in the *x*- and *y*-directions.

Wrinkle Edge Detection

The wrinkle edge detection is performed in three major steps. In the first step, an edge preserving smoothing technique called *adaptive smoothing*[8] is applied, which is based on anisotropic diffusion[9]. This is a non-linear, iterative algorithm that combines the sharpening of edges with smoothing of relatively uniform regions. Furthermore, we use a variant of adaptive smoothing described by Matalas, et al[10].

During each iteration, a weighted average in 3 x 3 neighborhoods of an image I is calculated, according to

$$I^{(t+1)}(x,y)=\frac{\sum_{i=-1}^{1}\sum_{j=-1}^{1} I^{(t)}(x+i,y+j)\,w^{(t)}(x+i,y+j)}{\sum_{i=-1}^{1}\sum_{j=-1}^{1} w^{(t)}(x+i,y+j)}, \quad (1)$$

where t is the iteration index. The weighting function, $w^{(t)}(x,y)$, for each pixel is calculated as

$$w^{(t)}(x,y)=e^{-\frac{G^2}{2k^2}}, \quad (2)$$

where

$$G=\max_{\substack{i=-1,0,1\\ j=-1,0,1}}\left(\left|I^{(t)}(x,y)-I^{(t)}(x-i,y-j)\right|\right). \quad (3)$$

The parameter k in (2) is used to set the gradient threshold where discontinuities are preserved. In this study, we have experimentally chosen k=5 and 10 iterations to be sufficient.

TEXTILE TOPICS
A research bulletin on fiber and textile industries.
Summer 2003 - Vol 2003-3

Published quarterly
Texas Tech University
International Textile Center
P.O. Box 45019
Lubbock, TX 79409-5019

The second step uses an edge detection technique based on Haralick's *cubic facet model*[6] to locate wrinkles. Around a center pixel and within a specified neighborhood, the facet model fits an underlying intensity image to a function f of a cubic polynomial in parametric form, where

(4) $$f(r,c) = k_1 + k_2 r + k_3 c + k_4 r^2 + k_5 rc + k_6 c^2 + k_7 r^3 + k_8 r^2 c + k_9 rc^2 + k_{10} c^3$$

The *IDDG operator*[7] uses the facet model coefficients $k_1 \ldots k_{10}$ to compute the integral of the directional derivative of f in the direction $\grave{e}$ (denoted as $F_{\grave{e}}$). $F_{\grave{e}}$ is maximized when

(5) $$\theta = \theta_{\max} = \tan^{-1}\frac{D_1}{D_2} = \tan^{-1}\frac{L^2 k_7 + \frac{1}{3}Lk_9 + k_2}{L^2 k_{10} + \frac{1}{3}Lk_8 + k_3},$$

where L is the window size and $\grave{e}_{max}$ is the direction of the maximum gradient[7,11]. The maximum gradient magnitude, F_{max}, is then calculated as

(6) $$F_{\max} = \sqrt{D_1^2 + D_2^2}\ .$$

We then check to see whether there is a negatively sloped zero crossing of the second directional derivative along the direction of the gradient. If the zero crossing is within the center pixel of the window, this pixel is marked as an edge point. Here we used a window size L=19 and gradient threshold F_{max}=0.3. The output of the IDDG operator provides a raw edge map that may contain small spurious edge points or slightly thicker edges than preferred. In the third and final step of this process, two algorithms are applied to *clean* the edge map. The first of these algorithms is morphological skeletonization, which thins the edges to one pixel wide. Next, connected component analysis allows for the removal of all objects less than n pixels in area. A minimum object size of n=15 was found to be sufficient for removing small spurious edges.

Feature Extraction

Using the resulting edge map, which identifies the wrinkle locations, we obtain cross-sections, or profiles, of the wrinkles at every edge point. For each edge point *(r,c)* in the edge map, two endpoints for the profile are calculated using

(7) $$(r_1, c_1) = (r + \frac{l}{2}\sin\theta, c + \frac{l}{2}\cos\theta)$$

and

(8) $$(r_2, c_2) = (r - \frac{l}{2}\sin\theta, c - \frac{l}{2}\cos\theta),$$

where l is the desired profile length and $\grave{e}$ is the direction of the maximum gradient obtained by the IDDG algorithm—$\grave{e}_{max}$ in (5). Then, using the adaptively smoothed image, the gray values of the pixels along the line from (r_1,c_1) to (r_2,c_2) are fit into an l-element vector using bilinear interpolation. This procedure results in the gray value of the edge point *(r,c)* to lie at the center of the profile. Figure 3 provides a visual example of this. Figure 3(a) shows an adaptively smoothed grayscale range image overlaid with the edge map (in white), while Figure 3(b) shows a close-up taken from the indicated section in Figure 3(a). The black line lying roughly perpendicular to the long, diagonal edge in Figure 3(b) indicates the location of one particular profile. We have experimentally chosen the profile length l=20 to provide a sufficient cross-section of the wrinkle.

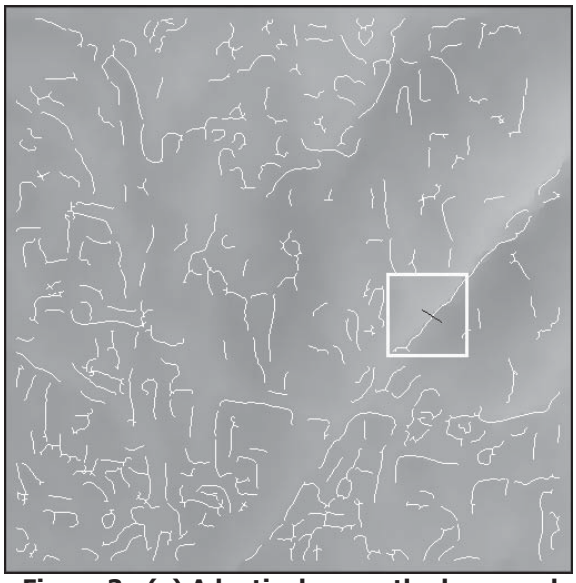

Figure 3: (a) Adaptively smoothed grayscale range image with edge map overlaid.

Figure 3: (b) Close-up of area indicated in (a) showing the location of a profile (black line) with respect to the edge (white line) at one particular edge point.

Thus far, we have examined two aspects of these profiles. The first is a profile's maximum amplitude, which is calculated as the difference of the maximum and the minimum gray values of the profile. This is an obvious choice for a feature, as it shows the height differences among the wrinkles. The second feature is a measurement of the shape, or transition, of the profile. First, to remove any height information, the profile is normalized so that the minimum value is zero and the maximum value is one. Next a derivative, or discrete difference, operator is applied to this normalized profile. Wrinkles with sharp transitions will produce high responses or spikes, while smooth wrinkles will produce a relatively 'flat' response. The measurement is then taken as a difference between the maximum and minimum values of this derivative. Figure 4 shows an example of these two measurements from the profile obtained in Figure 3. The maximum amplitude in Figure 4(a) is calculated to be 34 gray levels (rounded to the nearest integer), and the maximum amplitude of the derivative in Figure 4(b) is 0.68 (rounded to the nearest hundredth).

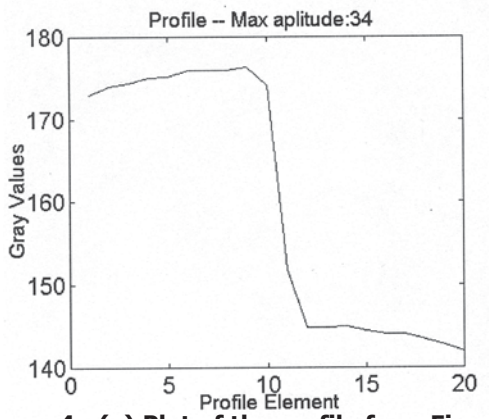

Figure 4: (a) Plot of the profile from Figure 3.

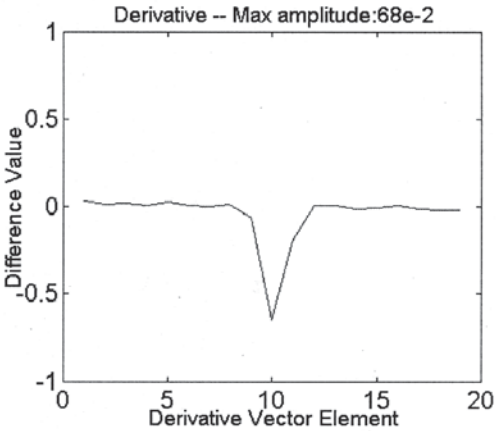

Figure 4: (b) Plot of the derivative of the *normalized* profile in (a).

After acquiring profiles at every edge point and calculating the two measurements for each profile, the results are examined using a 2-D histogram. Figure 5 shows one of these histograms for a fairly wrinkly swatch (AATCC grade of 2). The y-axis indicates increasing profile amplitude (increasing wrinkle height), while the x-axis represents increasing maximum amplitude of the derivative of the profile (increasing sharpness of the wrinkle). Lighter areas indicate higher counts. By observing these histograms, one can get an idea of the distribution of the various types of wrinkles in a particular fabric sample.

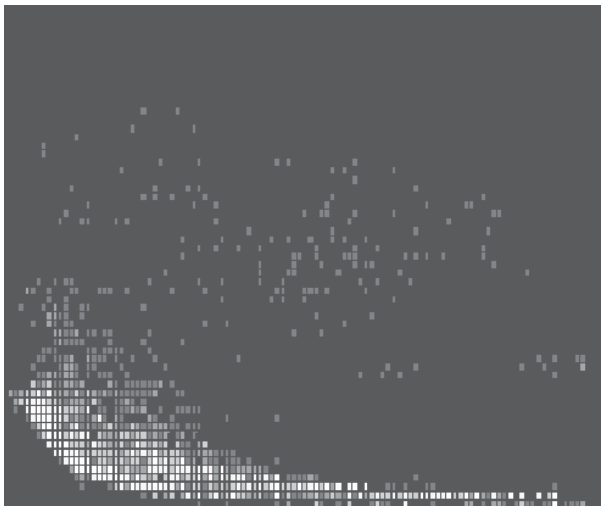

Figure 5: 2-D histogram of the two features. Lighter areas represent higher bin counts.

RESULTS

As a first step in the validation of this system, we have examined 26 different fabric samples. Three 15in. x 15in. swatches are cut from each of these samples and put through a standard laundering cycle as described by AATCC TM 124, providing a total of 78 test swatches. After the laundering process, the swatches are stored in a room at a specified temperature and humidity—also in accordance with AATCC procedures. In this same storage room, each fabric swatch is graded by technicians and then scanned using the laser-camera system. For scanning, a swatch is clipped onto the plexiglass platform, as shown in Figure 2. A total of four range images are acquired for each swatch. The first two are taken while the swatch is moved down and then back up. The second two range images are acquired by taking the swatch off, rotating it 90 degrees counterclockwise, and then clipping it back to the moving platform for another pair of up and down scans. This gives a total of 312 range images that were subsequently processed through the steps described above.

We feel that at this point there are two major factors that are paramount to validating the usefulness of this wrinkle profiling system, i.e. that it provides dependable quantification of wrinkles that appear on fabrics. The first of these factors examined here is consistency of the system in producing similar results for repeated scans of the same swatch regardless of scanning direction or orientation of the subject. For this, we looked at a histogram of the gradient magnitudes resulting from the IDDG operator (not to be confused with the 2-D feature histograms described earlier). Figure 6 shows one of these gradient magnitude histograms. Each line in the graph represents the same swatch scanned in each of the four different scanning positions. These plots are all very similar, indicating a high degree of repeatability regardless of scan direction or orientation. In fact, each downward scan is almost identical to the corresponding upward scan, which comes as no surprise since one image is essentially a vertically flipped version of the other. All other swatches show similar results with the variance of the distributions being lower for smooth samples and larger for wrinkled samples. The difference between the two pairs of the histograms of the scans before and after rotation in Figure 6 is attributed to the fact that some prominent wrinkles, due to their orientation with respect to the laser line, appear differently if sensed from a different angle. However, as will be shown later, this discrepancy does not have a significant effect on the ability to show similarity among the four scans of a swatch or among swatches from the same fabric sample.

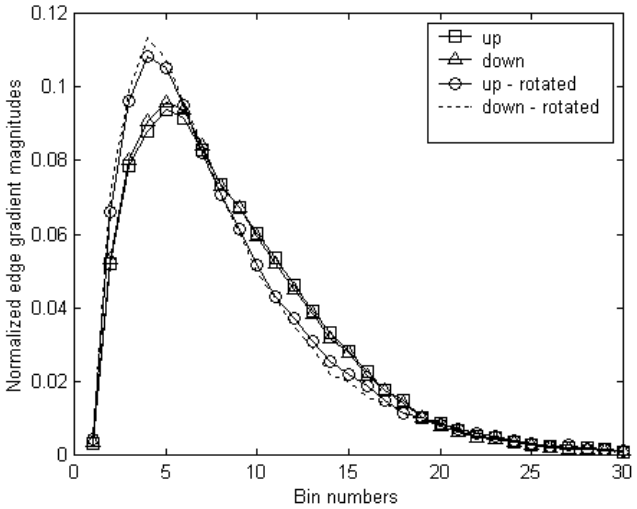

Figure 6 - Edge gradient histogram for the same swatch at four different scanning positions.

The next important aspect of this validation is to show that the system appropriately identifies wrinkles on a swatch and measures relevant features of those wrinkles. Using the AATCC smoothness grading system as a guide, Figure 7 shows three feature histograms of different samples with different grades. Figure 7(a) is a very wrinkly sample (AATCC grade 1) with a variety of different types of wrinkles. The grade-3 sample in Figure 7(b) shows mostly small wrinkles and creases with a few large ones. Finally Figure 7(c) is a very smooth, grade-5 fabric with almost no wrinkles at all. It is apparent from these graphs in Figure 7 that the system has the potential of describing a fabric's surface in much more detail than is offered by the current AATCC grading system.

Finally, as an analysis of both of these factors together, we looked at the similarity of the feature histograms from various swatches. For a measurement of similarity we calculate a mean squared error (MSE) between two histograms as

$$e = \frac{\sum_{x,y} \left(H_1(x,y) - H_2(x,y)\right)^2}{N},$$

where the differences of each bin, *(x,y)*, in each histogram, H_1 and H_2, are squared, summed, and then divided by N, the total number of bins. Table 1 shows the mean squared error of five different swatches being examined versus each other. Three of these swatches—S1-1, S1-2, and S1-3—come from the same fabric sample. (Refer to Table 2 for the technicians' AATCC grades of these swatches). The swatch labeled S1-1-iron represents swatch S1-1 after it has been ironed and subsequently re-scanned. Finally, S2-1 is a swatch from a different fabric. (The feature histogram for S2-1 is shown in Figure 5(c).) Also, each swatch is represented by two of the aforementioned scans: the downward scan and the downward scan with the swatch rotated ninety degrees from its original position (denoted by "-rot"). As indicated by the shaded regions, there is a high degree of similarity, or relatively low MSE, among the scans of the same swatch and also among the three swatches S1-1, S1-2, and S1-3. This strongly indicates consistency not only across different scans of the same swatch, as discussed earlier, but also among swatches from the same fabric sample. In fact, the average *intra*-sample MSE among the 12 images for each of the 26 fabric samples (four scans of each of the three swatches per fabric) is 5.9 with a standard deviation of 3.2. (The intra-sample averages were calculated by looking at the unique permutations of the 12 images versus each other but leaving out the

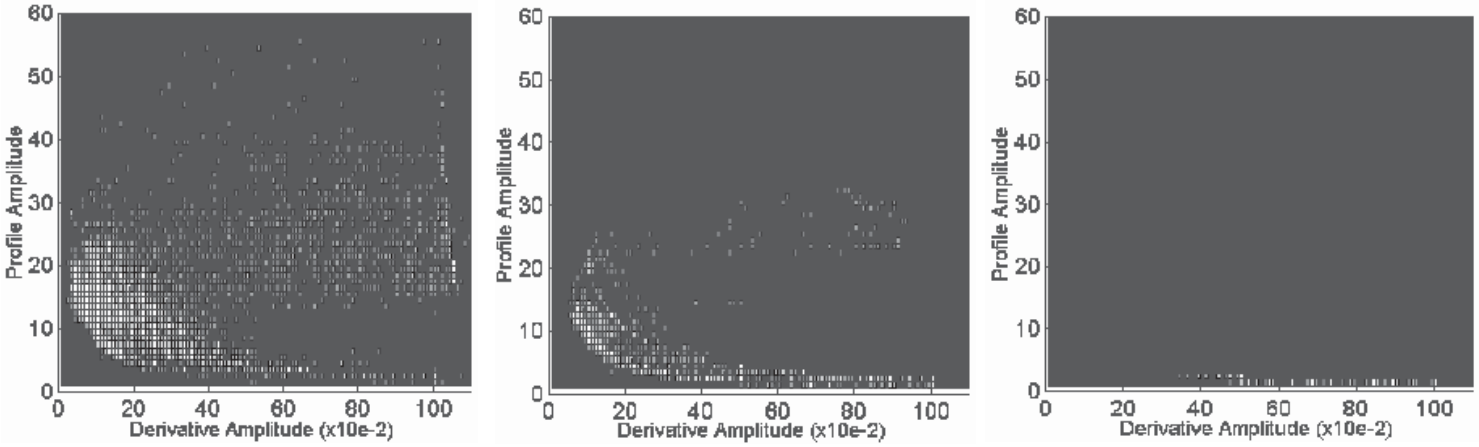

Figure 7 - Feature histograms for three different samples. AATCC grades for these three samples are (a) 1, (b) 3, and (c) 5.

	S1-1-iron	S1-1-Iron-rot.	S1-1	S1-1-rot.	S1-2	S1-2-rot.	S1-3	S1-3-rot.	S2-1	S2-1-rot.
S1-1-iron	0.0	3.8	16.3	22.7	16.0	19.8	18.7	18.0	10.2	8.4
S1-1-iron-rot.	3.8	0.0	28.8	35.1	28.5	30.9	29.5	29.4	23.1	20.3
S1-1	16.3	28.8	0.0	4.5	1.0	4.7	3.9	3.3	12.4	12.5
S1-1-rot.	22.7	35.1	4.5	0.0	4.4	3.0	7.2	2.0	18.7	18.7
S1-2	16.0	28.5	1.0	4.4	0.0	4.0	3.0	3.1	12.7	12.7
S1-2-rot.	19.8	30.1	4.7	3.0	4.0	0.0	3.4	1.7	19.8	19.7
S1-3	18.7	29.7	3.9	7.2	3.0	3.4	0.0	3.7	19.2	19.1
S1-3-rot.	18.0	29.4	3.3	2.0	3.1	1.7	3.7	0.0	15.9	15.8
S2-1	10.2	23.1	12.4	18.7	12.7	19.8	19.2	15.9	0.0	0.6
S2-1-rot.	8.4	20.3	12.5	18.7	12.7	19.7	19.1	15.8	0.6	0.0

Table 1: Mean squared error of five different swatches versus each other at two scanning positions each. The shaded regions indicate a high degree of similarity.

combinations of an image versus the same image—in which case the MSE would be 0.) Furthermore, the average *inter*-sample MSE –12 scans of one fabric compared with the 12 scans of a different fabric—is 11.7 with a standard deviation of 8.2.

CONCLUSIONS / FUTURE WORK

Fabric smoothness is, to the textile industry, one of the most important factors in judging the aesthetic appeal of fabrics. However, as stated before, the current smoothness grading system is seriously lacking in its ability to adequately and effectively evaluate this quality measurement. For example, one of the most notorious shortcomings of AATCC TM 124 is lack of agreement among the technicians' grades. The three swatches S1-1, S1-2, and S1-3 in the previous example involving Table 1 were given a grade of 2 by one technician and then a grade of 3 by the other two technicians (see Table 2). This difference of one grade level is egregious given that there are only six possible grades. This disparity also alludes to another problem with the grading system: subjectivity. Furthermore, in accordance with AATCC standards these readings are averaged to produce an actual grade of 2.67. This application of a linear operator, such as a mean, to a set of grades that are not linear (i.e. with possible values of 1, 2, 3, 3.5, 4, and 5—which are not based on any scientific measurements) really has very little meaning. For these reasons and others, we feel that the textile industry is in need of a system, such as the one proposed, that provides reliable measurements of wrinkles for smoothness evaluation of fabrics.

	Tech. 1	Tech.2	Tech. 3
S1-1	2	3	3
S1-2	2	3	3
S1-3	2	3	3

Table 2: Technician's grades of swatches S1-1, S1-2, and S1-3 discussed in Table 1

The results shown here of the preliminary testing of this system indicate that it is indeed capable of overcoming the deficiencies of the current grading system. The examples given in Figure 6 and Table 1 show that the output of the system is very consistent among repeated scans of the same swatch as well as among swatches from the same fabric sample. This is further proven by the mean of the intra-sample MSE among all 26 sample fabrics being so low (5.9) and relatively narrow in distribution (std. dev. 3.2). Furthermore, knowing the diversity of the samples chosen for the study and given the wide distribution of the inter-sample MSE discussed in section 4, it is clear that the system is able to discern among a wide variety of sample fabrics.

As this preliminary study concludes, we have shown that the designed system, as a measuring device, is highly capable of comparing the smoothness of fabric specimens to one another. However, given that the final result of the system is not a "grade", one might ask: how could it replace the current grading system? There are many specific applications within the textiles industry that would be best served by tailoring this system to meet their needs. For example, in the continuation of our research, we plan on devising a study making use of chemicals that reduce wrinkling, called finishes. These chemicals are applied to fabrics in varying strengths with the idea that more concentrated solutions further reduce wrinkling. Currently, chemists researching new finishes that are less expensive and more environmentally-friendly rely on technicians using the AATCC grading scale as a measure for their effectiveness. However, we believe that with this wrinkle profiling system, we will be able to discern differences among varying solution strengths with much greater accuracy than is provided by the AATCC smoothness grading system.

REFERENCES

1 AATCC Technical Manual, 1991, p288.

2 B. Xu, and J.A. Reed, "Instrumental Evaluation of Fabric Wrinkle Recovery," J. Text. Inst., 1995, 86(1), p129.

3 J. Su and B. Xu, "Fabric Wrinkle Evaluation Using Laser Triangulation and Neural Network Classifier," Optical Engineering, 1999, 38 (10), p1688.

4 T.J. Kang, D.H. Cho, S.M. Kim, "New Objective Evaluation of Fabric Smoothness appearance," Text. Res. J. 2001, 71(5), p446.

5 C. Turner, H. Sari-Sarraf, A. Zhu, E. Hequet, S. Lee, "Automatic Assessment of Fabric Smoothness," *IEEE Midwest Conf. on Circ. and Syst.*, 2002.

6 R.M. Haralick, "Digital Step Edges From Zero Crossings of Second Directional Derivatives," *IEEE Trans. Pattern Analysis and Machine Intelligence*, vol. 6, 1984.

7 O.A. Zuniga and R.M. Haralick, "Integrated Directional Derivative Gradient Operator," *IEEE Trans. Syst. Man Cybern.*, vol. 17, 1987.

8 P. Saint-Marc, J. Chen, and G. Medioni, "Adaptive Smoothing: A General Tool for Early Vision," *IEEE Trans. Pattern Analysis and Machine Intelligence*, vol. 13, 1991.

9 P. Perona and J. Malik, "Scale-Space and Edge Detection Using Anisotropic Diffusion," *IEEE Trans. Pattern Analysis and Machine Intelligence*, vol. 12, 1990.

10 I. Matalas, R. Benjamin, R. Kitney "An Edge Detection Technique Using the Facet Model and Parameterized Relaxation Labeling". *IEEE Trans. Pattern Analysis and Machine Intelligence*, vol. 19, 1997.

11 R.M. Haralick and L.G. Shapiro, *Computer and Robot Vision*, vol. 1. Reading, Mass.: Addison-Wesley, 1992.